

Feasibility and safety of pulsed field ablation at the ventricular outflow tract using focal point catheter

Lihui Zheng, MD, PhD,¹ Pakezhati Maimaitijiang, MD,¹ Aiyue Chen, MD, Zihao Lai, MD, Yan Yao, MD, PhD, FHRS

ABSTRACT

BACKGROUND Ventricular arrhythmias commonly originate from the ventricular outflow tract. It remains unexplored whether pulsed field ablation (PFA) can create durable lesions safely at the ventricular outflow tract.

OBJECTIVE This study aimed to evaluate the feasibility and safety of a novel PFA catheter to deliver focal ablation to the ventricular outflow tract, especially pulmonary and aortic sinus cusps (PSCs and ASCs).

METHODS Twelve swine were divided into 3 groups: 24-hour, 2-week, and 4-week post-ablation. PFA was delivered to predefined sites of PSCs and ASCs with a focal point catheter, positioned by a mapping system, fluoroscopy, and intracardiac echocardiography. Electrophysiologic assessment, coronary angiography, transesophageal echocardiography, and gross and histologic examination were performed to evaluate the impact of PFA delivery on cardiac structure and function.

RESULTS All subjects survived, and no adverse events were observed. There was a significant decrease in voltage amplitude and increase in pacing thresholds at PSCs and ASCs. There were no significant differences in AH or HV intervals between pre-ablation and post-ablation (AH, $P = .70$; HV, $P = .90$). After PFA delivery to ASCs, coronary arteries were fully perfused in each heart, without ST-segment elevation observed. No severe valvular dysfunction was observed on intracardiac echocardiography and transesophageal echocardiography. Gross and histologic examination confirmed the creation of well-demarcated lesions at the targeted sites without damage to adjacent structures.

CONCLUSION PFA delivered by the focal point catheter could create durable lesions at PSCs and ASCs without damage to coronary arteries, atrioventricular block, or valvular dysfunction, indicative of the feasibility and safety of this novel PFA catheter at the ventricular outflow tract.

KEYWORDS Pulsed field ablation; Ventricular outflow tract; Pulmonary sinus cusp; Aortic sinus cusp; Feasibility; Safety

(Heart Rhythm 2024; ■:1–10) © 2024 Heart Rhythm Society. All rights are reserved, including those for text and data mining, AI training, and similar technologies.

Introduction

The outflow tract is the most common location of origin for ventricular arrhythmias (VAs), especially premature ventricular complexes (PVCs) and idiopathic ventricular tachycardia (VT), in patients without structural heart disease.^{1,2} Outflow tract VT is a form of idiopathic VT that arises from the outflow tract of the right or left ventricle or aortic cusps.³ Catheter ablation is a highly recommended treatment strategy for these conditions.^{4,5} Unlike the right ventricular outflow tract (RVOT), where catheter delivery to the pulmonary sinus

cusps (PSCs) often necessitates the reversed U-curve technique to achieve better catheter to tissue contact, the left ventricular outflow tract (LVOT) poses unique challenges because of its proximity to the aortic root, coronary artery ostia, and cardiac conduction bundle.⁵ Thus, ablation within the aortic sinus cusps (ASCs) is more complicated with higher risk. Conventional energy sources like radiofrequency (RF) ablation within these cusps could result in some complications, such as coronary artery injury, atrioventricular block, or valvular dysfunction.

¹From the Arrhythmia Center, Fuwai Hospital, National Center for Cardiovascular Diseases, Chinese Academy of Medical Sciences and Peking Union Medical College, Beijing, China.

¹Drs Zheng and Maimaitijiang are first co-authors.

Pulsed field ablation (PFA) represents a novel, nonthermal modality capable of inducing irreversible electroporation of cell membranes through subsecond electrical impulses.^{6,7} Myocytes exhibit a lower characteristic threshold for irreversible electroporation compared with adjacent cell types, positioning PFA as a superior alternative to RF ablation by ensuring tissue-specific cell death while preserving the integrity of surrounding tissues.⁸ Despite its established effectiveness and safety in treating atrial arrhythmias, use of PFA for VT originating from the ventricular outflow tract remains unexplored. This study used a novel PFA system to characterize the feasibility and safety of PFA deliveries to the RVOT and LVOT, especially PSCs and ASCs, in a preclinical porcine model.

Methods

This preclinical study was approved by the Institutional Animal Care and Use Committee and conformed to the position of the Chinese Heart Association on research animal use. The study was performed at the Key Laboratory of Silversnake (Yinshe) Clinical Center in Guangzhou, Guangdong Province, China. The research has adhered to the *Guide for the Care and Use of Laboratory Animals*.

PFA ablation system

The PFA system consists of a PFA generator (NanoAblate; EnChannel Medical, Guangzhou, China) and a novel 7F steerable, dual-purpose PFA catheter (PFLine [EnChannel Medical]; Figure 1A). The PFA catheter includes 3 electrodes: focal PFA by activation of electrodes 1–2 or 2–3 and linear ablation by activation of electrodes 1–3 (Figure 1B). When introduced into the cardiac chamber, the bidirectional catheter allows 0°–180° deflection to either side with accurate catheter tracking. PFA is applied by a biphasic waveform of microsecond scale with an output of ± 750 V and an application duration of 4 seconds.

Experimental protocol

A total of 12 Yorkshire swine (weighing 45–50 kg) were evenly divided into 3 survival subgroups: 24-hour post-ablation, 2-week post-ablation, and 4-week post-ablation. After each survival period, animals were sacrificed to assess the ventricular tissue response to electroporation. The animals were prepared

under general anesthesia with isoflurane inhalation and mechanical ventilation. Vascular access was established with standard 7F sheaths inserted percutaneously in the femoral artery and vein. Heart rate and femoral artery blood pressure were monitored alongside standard electrocardiographic leads and intracardiac electrogram recording. Heparinized saline was used to prevent intraprocedural clotting, aiming

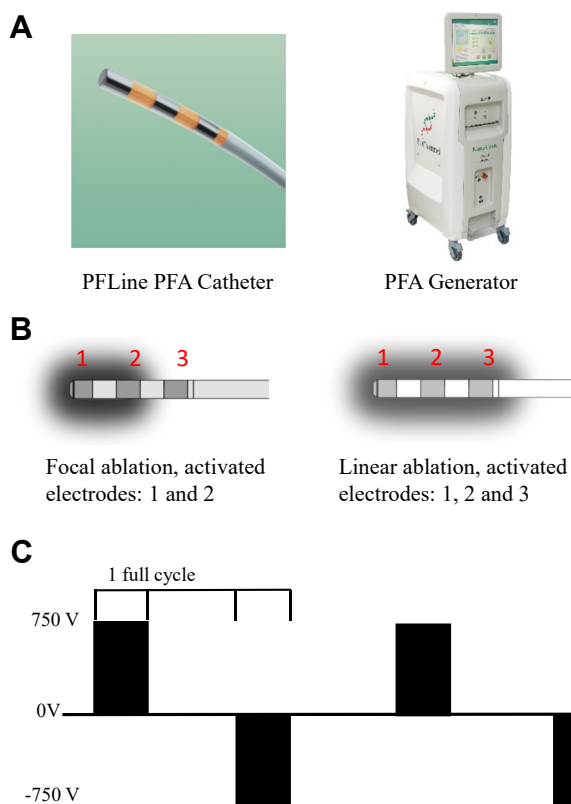


Figure 1

PFLine pulsed field ablation (PFA) system. A: PFLine PFA catheter and generator. B: Dual ablation modes: the focal ablation mode (activating electrodes 1 and 2) and the linear ablation mode (activating electrodes 1, 2, and 3). C: PFA is delivered by a biphasic waveform of microsecond scale with an output of ± 750 V and application duration of 4 seconds including multiple trains of biphasic bipolar pulses.

for an activated clotting time of 200–300 seconds. Cefazolin (1000 mg) was given intravenously during the procedure, followed by oral cefpodoxime (10 mg/kg) after the procedure to prevent infection in the long-term studies.

The PFA catheter was precisely positioned with fluoroscopy guidance, intracardiac echocardiography (ICE; Abbott Cardiovascular, Plymouth, MN), local ventricular electrograms, and a 3-dimensional (3D) mapping system (Figure 2). Detailed electroanatomic mapping of the ventricles through retroaortic access, including the PSCs and ASCs, was performed with the EnSite NavX mapping system (Abbott). The PFA ablation catheter, employing fast anatomic mapping techniques, created 3D maps of the entire ventricle.

The ICE catheter was placed either in the right atrium or within the right ventricular inflow area, facilitating visualization of the aortic valve, pulmonary valve, and PSCs. For ablations in the ASCs, the left main and right coronary ostia were visualized simultaneously, maintaining a safe distance from the ablation catheter tip to the coronary ostium in the long-axis view.

The PFA catheter was inserted in the right femoral vein through a steerable long sheath (Agilis; Abbott) and advanced to the right ventricle. Mapping focused on the RVOT region beneath the pulmonary artery (PA), including 6 cross-sectional segments: posteroseptal, mid septal, anteroseptal, posterior free wall, mid free wall, and anterior free wall. The

Abbreviations

AC:	anterior cusp
ASC:	aortic sinus cusp
LC:	left cusp
LCC:	left coronary cusp
NCC:	noncoronary cusp
PFA:	pulsed field ablation
PSC:	pulmonary sinus cusp
RC:	right cusp
RCC:	right coronary cusp

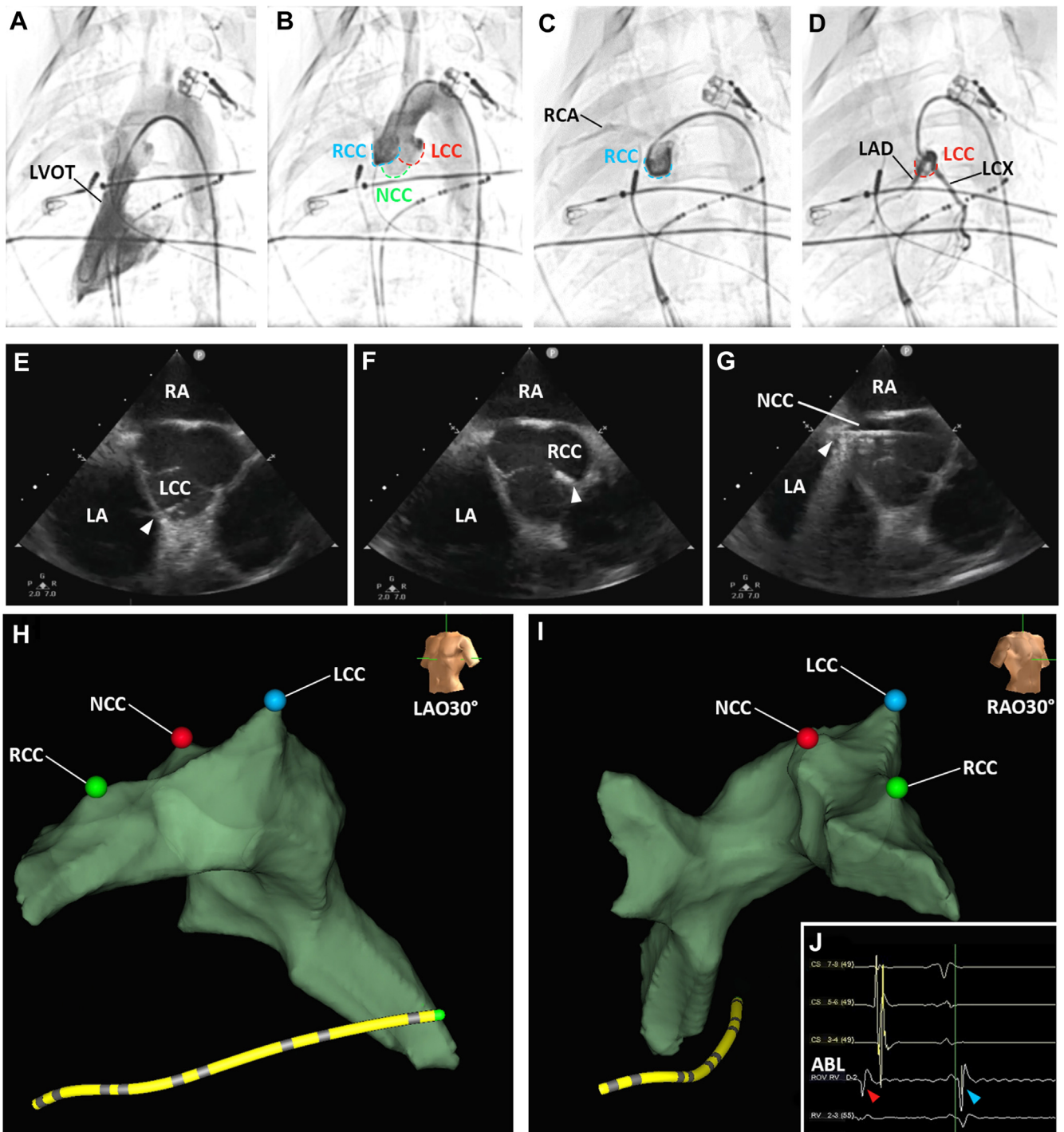


Figure 2

Left ventricular outflow tract (LVOT) imaging during pulsed field ablation (PFA) delivery. A, B: Fluoroscopy was performed when the tip of the catheter was located at the LVOT (A), and the aortic sinus cusps were visualized (B). C, D: Coronary angiography was repeated after PFA delivery. E–G: Based on intracardiac echocardiography, the tip of the PFA catheter (arrowhead) was located at left coronary sinus cusp (LCC), right coronary sinus cusp (RCC), and noncoronary sinus cusp (NCC). H, I: The location of each ablation site of aortic sinus cusps is shown in the left anterior oblique (LAO) and right anterior oblique (RAO) 30° view by the 3-dimensional mapping system. J: The electrogram was recorded when the tip of the ablation catheter (ABL) was located at NCC. LA = left atrium; LAD = left anterior descending artery; LCX = left circumflex artery; RA = right atrium; RCA = right coronary artery.

PA and these PSCs—the left cusp (LC), right cusp (RC), and anterior cusp (AC)—are presented in the detailed mapping (Figure 3).

Ablation sites were selected on the basis of the ability to position the catheter perpendicular or nearly perpendicular

to the tissue. One ablation site per sinus cusp was performed under the guidance of 3D mapping and ICE to allow exact evaluation of the depth and length of the lesion and its impact on the surrounding tissues. After completion of ablation at each sinus cusp, the catheter was withdrawn to check for

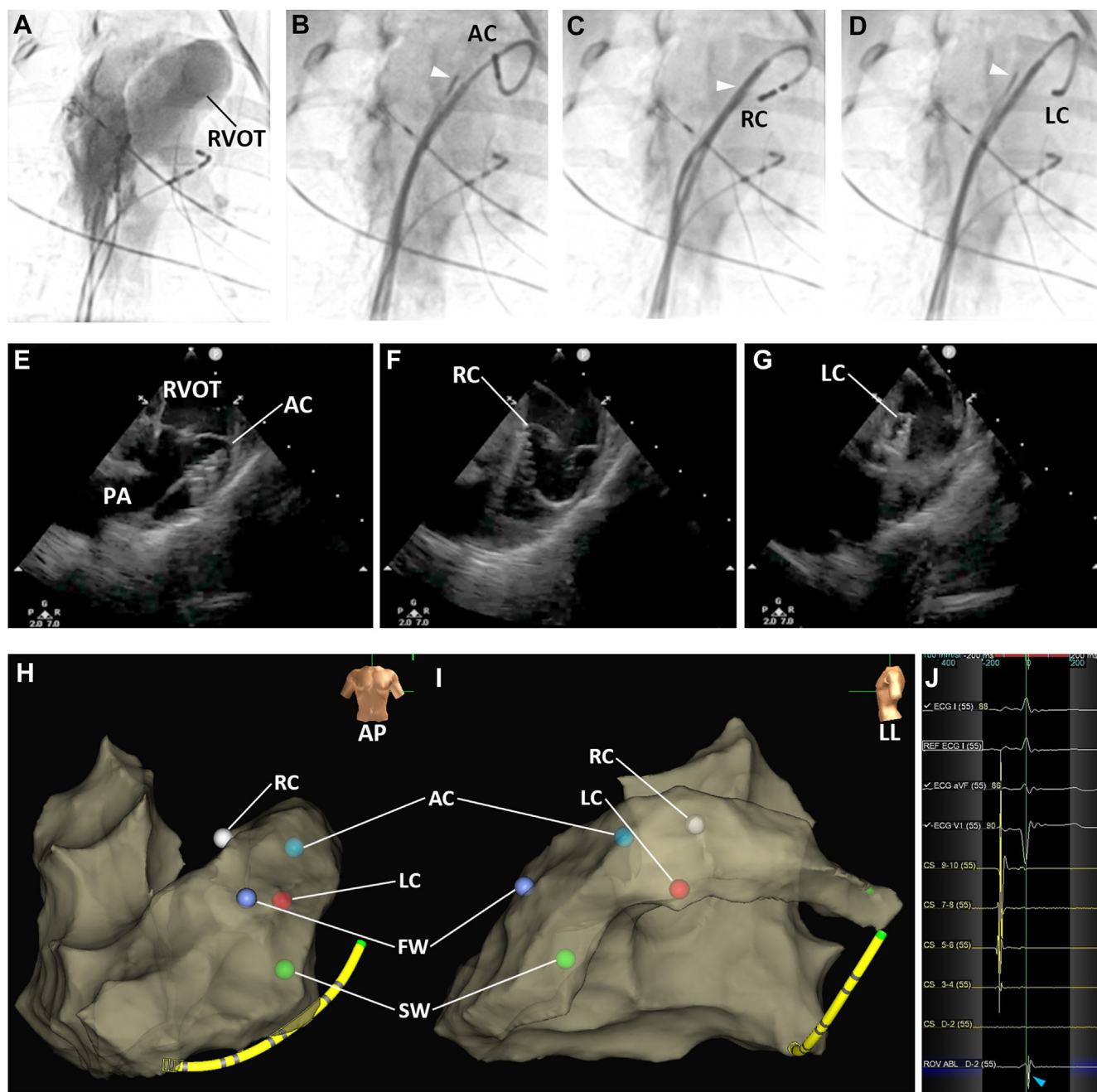


Figure 3

Right ventricular outflow tract (RVOT) imaging during pulsed field ablation (PFA) delivery. A–D: Fluoroscopy was performed at the RVOT (A), and the position of the PFA catheter and the tip of the intracardiac echocardiography (ICE) catheter (arrowhead) were visualized (B–D) at anterior cusp (AC), right cusp (RC), and left cusp (LC). E–G: On ICE at the RVOT, the tip of the PFA catheter was located at AC, RC, and LC. H, I: The location of each ablation site of pulmonary sinus cusps as well as free wall (FW) and septal wall (SW) is shown in the anterior posterior (AP) and left lateral (LL) view by the 3-dimensional mapping system. J: The electrogram was recorded. PA = pulmonary artery.

any signs of charring or thrombus formation. A single application was administered at each predefined ablation site. Electrograms, bipolar voltage amplitude, and pacing thresholds (PTs), defined as the lowest voltage when consistent capture (>3 times) of the entire chamber was observed in response to pacing, were recorded before and after ablation. The PTs after ablation would be underestimated as 8 V if ventricular rhythm could not be captured with the maximal pacing voltage.

Before mapping above the aortic valve, selective angiography of the coronary arteries and aorta was performed to determine the location of the coronary artery ostia and to make sure that coronary arteries were fully perfused. PFA applications were maintained at a minimum distance of 5 mm from the coronary artery ostium for safety purposes. Coronary angiography was also performed after PFA delivery, and it would be repeated immediately if significant ST-T-segment changes were observed. Electrophysiologic parameters,

including heart cycle length, AH interval, HV interval, and atrioventricular node Wenckebach point, were documented before and after PFA ablation. Transesophageal echocardiography (TEE; Vivid E9, GE Health Care, Chicago, IL) was performed on each heart before cardiac tissue extraction to evaluate the pulmonary and aortic valve function.^{9,10} Cardiac function abnormalities were also assessed with echocardiography.

Histopathologic analysis

The heart, pericardium, and lungs were excised en bloc and examined for injury. The left coronary artery was cannulated with a small flexible probe, and the left anterior descending and left circumflex arteries were inspected for damage. The heart was excised, and the ventricles were opened along the long axis. Ablation lesions were identified and photographed during gross pathologic examination. After any abnormalities or injuries were documented, tissues were preserved in 10% neutral buffered formalin for histologic analysis. Hematoxylin-eosin and Masson trichrome staining was performed to assess tissue structure and ablation damage. Lesion continuity and depth were evaluated for each slide by 2 investigators independently. Discrepancies were discussed with a senior cardiologist until a consensus was reached.

Statistical analysis

Continuous variables were expressed as mean values and standard deviations, and categorical parameters were presented as percentages. The paired Student *t*-test was performed to compare the continuous variables between pre-ablation and post-ablation. A 2-sided *P* value of <.05 was considered statistically significant. The R statistical software (version 4.2.3; R Foundation for Statistical Computing, Vienna, Austria) was used to perform all the statistical analysis.

Results

A total of 12 swine were treated with the novel PFA catheter that was delivered successfully to each PSC and ASC site, except for the AC and LC in 2 swine, which were unreachable because of anatomic variations in the PA. No waveform interruptions or muscle contractions were observed when PFA was delivered according to the protocol. No microbubbles were observed with ICE during the procedures. All animals survived with no VT detected.

Feasibility evaluation

Electrophysiologic assessment

After application of PFA, there was a significant reduction in bipolar voltage amplitude at each ASC ablation site compared with before ablation (Supplemental Table; Figure 4B; noncoronary cusp [NCC], *P* < .001; right coronary cusp [RCC], *P* = .004; left coronary cusp [LCC], *P* = .006). Similarly, statistically significant changes in voltage amplitude

before and after ablation were observed at each PSC site (Supplemental Table; Figure 4A; AC, *P* < .001; RC, *P* = .005; LC, *P* = .017) as well as at the septal and free wall of the RVOT (septal wall, *P* = .002; free wall, *P* < .001).

There was a substantial increase in PTs after ablation at each ablation site of ASCs (NCC, *P* = .003; RCC, *P* < .001; LCC, *P* = .004), PSCs (AC, *P* = .011; RC, *P* < .001; LC, *P* < .001), and septal wall (*P* < .001) and free wall (*P* < .001) of RVOT in relation to those before ablation. Seven ablation sites of ASCs and PSCs were generated (NCC, *n* = 1; RCC, *n* = 2; LCC, *n* = 1; AC, *n* = 1; RC, *n* = 2) without ventricular capture before and after ablation using the maximal voltage. To mitigate data loss, pre-ablation and post-ablation PTs of these sites were underestimated to be 8 V equally, meaning that there was no difference in PTs between pre-ablation and post-ablation. The elevation of PTs at each ablation site of ASCs and PSCs was relatively lower than before, but the changes in PTs were still statistically significant (Supplemental Table; Figure 4C and 4D; NCC, *P* = .004; RCC, *P* = .001; LCC, *P* = .005; AC, *P* = .013; RC, *P* = .001; LC, *P* < .001).

Gross and histologic examination

At 24 hours after ablation, PFA delivery to the ASCs (Figure 5C and 5D) and PSCs (Figure 6A and 6B) resulted in well-demarcated lesions with a depth of 3.9 ± 0.9 mm and 4.3 ± 1.2 mm, respectively (Table 1). Histologic examination indicated that transverse striations of the myocardium after ablation became indiscernible with sarcoplasmic coagulation and mild inflammatory cell infiltration (Figures 5B and 6C). Of note, PFA application to the NCC also resulted in observable damage to the right atrium (Figure 5A).

The ablated myocardium was resolved in the 2-week post-ablation group with wide-ranging replacement granulation tissue and vascular formation (Figure 6D and 6E). The mean depth for the lesions 2 weeks after ablation was 3.6 ± 1.1 mm for the ASCs and 3.8 ± 0.6 mm for the PSCs (Table 1).

In the 4-week post-ablation group, widespread and uninterrupted replacement fibrosis was observed with a depth of 3.7 ± 1.0 mm and 3.6 ± 0.4 mm for the ASCs and PSCs, respectively (Figure 6F). Uniform and transmural lesions were observed in the free wall of RVOT (mean depth, 3.5 ± 1.1 mm), and wide-ranging replacement fibrosis was also observed in the septal wall of RVOT 4 weeks after ablation (Supplemental Figure).

Safety evaluation

Atrioventricular conduction assessment

There were no significant differences in atrium to His (AH), His to ventricle (HV), atrioventricular (AV), and ventricle to ventricle (VV) intervals between pre-ablation and post-ablation (AH, *P* = .70; HV, *P* = .90; AV, *P* = .76; VV, *P* = .84; Figure 7), indicating no atrioventricular block occurred after PFA delivery. Histologic examination of the ablated sites of NCC demonstrated no collateral damage to the nerves and critical components of cardiac conduction bundles, whereas

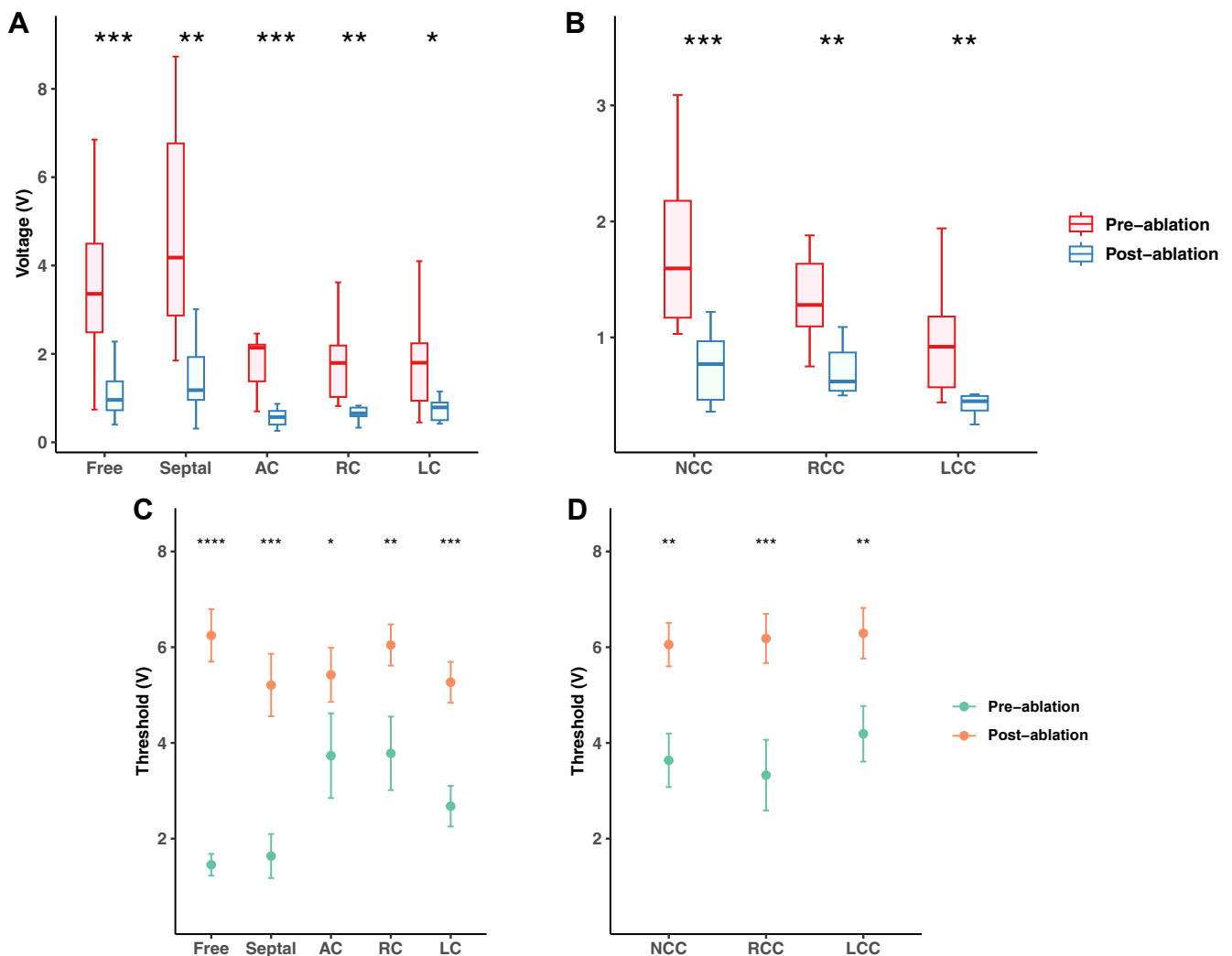


Figure 4

Changes in voltage amplitude and pacing thresholds between pre-ablation and post-ablation. **A, B:** The voltage amplitude was significantly reduced at each ablation site of right and left ventricular outflow tracts. **C, D:** The pacing thresholds were significantly elevated at each ablation site of right and left ventricular outflow tracts. AC = anterior cusp; LC = left cusp; LCC = left coronary sinus cusp; NCC = noncoronary sinus cusp; RC = right cusp; RCC = right coronary sinus cusp.

the surrounding myocytes were impaired or replaced with fibrotic tissue (Figure 5B and 5G).

Vascular assessment

After PFA delivery to the ASCs, especially LCC and RCC, the left and right coronary arteries assessed with angiography were fully perfused with normal blood flow, similar to those before ablation. Moreover, all animals experienced no ST-segment elevation after ablation. There was no evidence of vascular stenosis or intimal thickening in transverse sections of the coronary arteries. No collateral damage to small arteries or arterioles within fibrotic zones was observed during the acute and chronic phase after ablation (Figure 5E and 5G; Figure 6C).

Valvular assessment

Based on ICE imaging, no valvular dysfunction during ablation was observed, and the motion of aortic and pulmonary valves

was normal after PFA delivery. TEE with color Doppler was performed in the 4-week post-ablation group. There was no aortic regurgitation, and mild pulmonic regurgitation was observed in 1 of the 4 animals (regurgitant orifice area, 0.6 cm²). Based on the histologic examination, there was no evidence of collateral damage to the valve leaflets or the fibrous skeleton of both valves (Figure 5F).

Discussion

To our best knowledge, this is the first preclinical study to evaluate the safety and effectiveness of this novel PFA catheter at RVOT and LVOT in a porcine model. PFA is a new ablative therapy for cardiac arrhythmias. However, there are limited data on the application of PFA to VAs. A case of acutely effective ablation of PVCs using multielectrode pulsed field electroporation (PFE) in the RVOT and a case of acutely effective endocardial focal PFE of apparent epicardial VT were recently published.^{11,12} Neither study reported durability and follow-up. Worck and coworkers¹³ reported a case

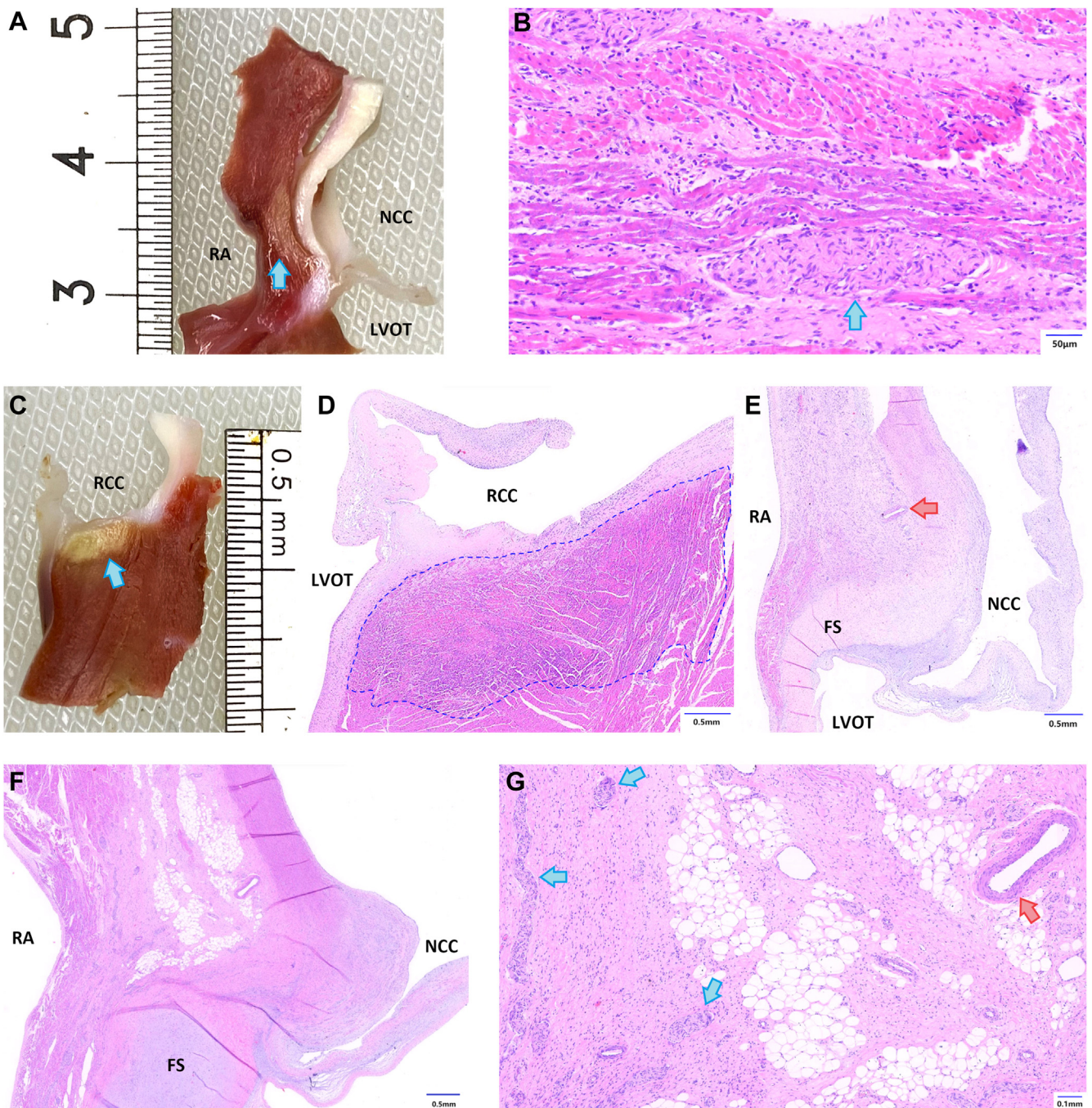


Figure 5

Gross pathologic and histologic examination of pulsed field ablation (PFA) lesions at left ventricular outflow tract (LVOT). A, B: The PFA lesion (arrow) at noncoronary cusp (NCC) 24 hours after ablation (A), showing (B) no collateral damage to the nerve (arrow) with the surrounding myocytes impaired. C, D: The well-demarcated lesion (arrow) at right coronary cusp (RCC) 24 hours after ablation. E: Histology of the PFA lesion at NCC after 2 weeks of survival without impact on the small artery (red arrow). F, G: The PFA lesion at NCC 4 weeks after ablation (F), showing (G) no collateral damage to the nerves (blue arrows) and arteries (red arrow). FS = fibrous skeleton; RA = right atrium.

of focal PFE treatment of outflow tract premature ventricular contractions with 2 months of antiarrhythmic drug-free follow-up, showing that safe and durable eradication of PVCs originating in the ventricular outflow tract is feasible with focal PFE. However, electroporation was applied solely to the RVOT.¹³

In this study, we examined a novel PFA catheter and waveform to demonstrate that durable lesions could be created

without causing collateral damage to coronary arteries, inducing atrioventricular block, or impairing valvular function. It was indicative of the safety and feasibility of this PFA catheter used at RVOT and LVOT, especially PSCs and ASCs. Thus, this study would expand our knowledge concerning PFA in the ablation of VAs.

The enhanced PTs and reduced voltage amplitude were observed at each ablation site of ASCs and PSCs, suggesting

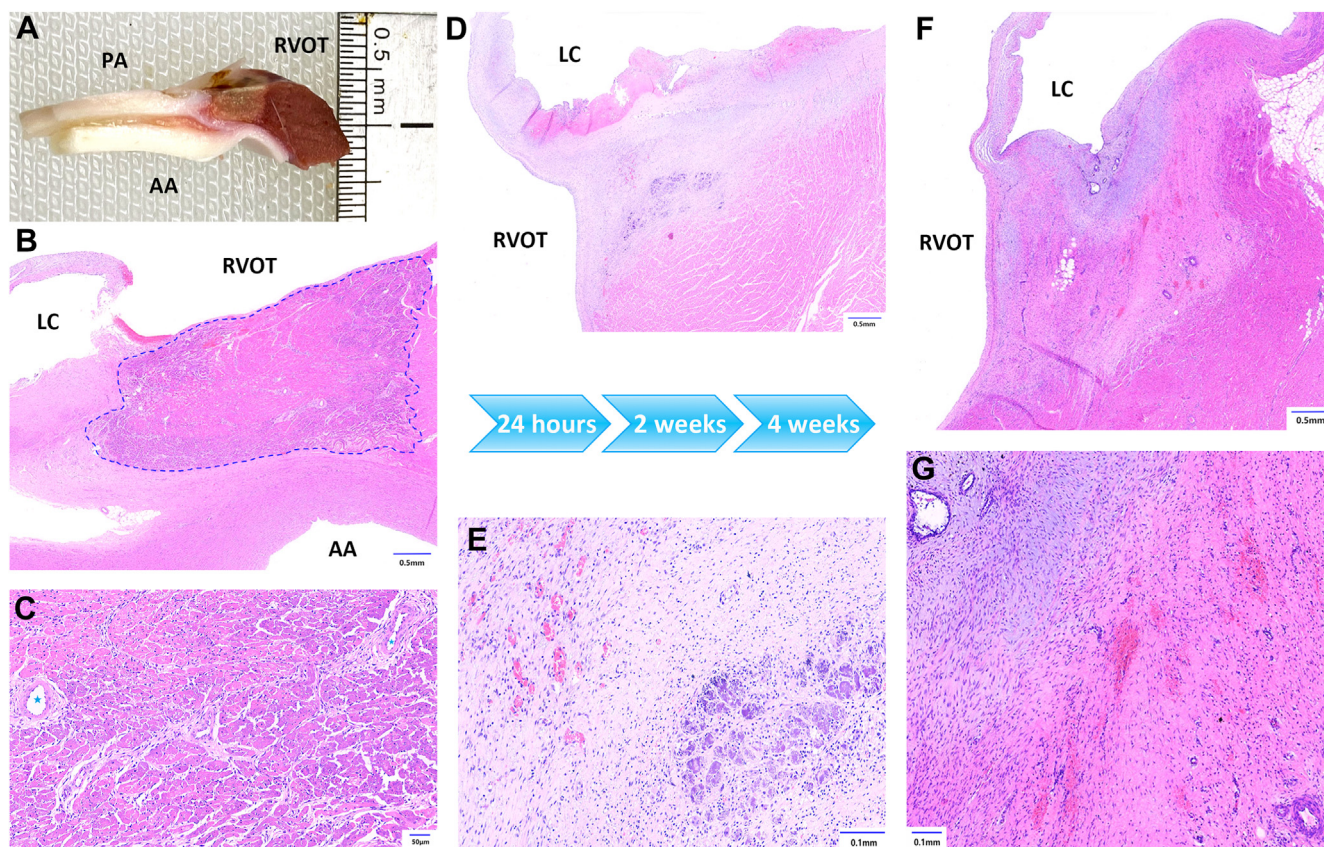


Figure 6

Gross and histologic examination of pulsed field ablation (PFA) lesions at pulmonary sinus cusps. A–C: The well-demarcated lesion at left cusp (LC) after 24 hours of survival (A, B), showing (C) no collateral damage to arterioles (star). D, E: Histology slide for the PFA lesion in the 2-week post-ablation group (D), and (E) the ablated myocardium was resolved with replacement granulation tissue and vascular formation. F, G: The PFA lesion at LC 4 weeks after ablation (F), showing (G) uninterrupted replacement fibrosis. AA = ascending aorta; PA = pulmonary artery; RVOT = right ventricular outflow tract.

the potential of these electrophysiologic changes as early indicators of lesion formation. Based on gross and histologic examination, acute and chronic lesions were well demarcated with a mean depth of 3.6 to 4.3 mm. It has recently been reported that point PFA lesions with an average depth of 5.6–8.1 mm were created for common idiopathic VA locations, where a custom PFA generator and a monopolar waveform were used to deliver 2000 V with 10 packets per application and 4 applica-

tions per site.^{14,15} In addition, deeper lesions could be created when PFA was delivered with application repetition.¹⁶ In this study, an output of ± 750 V with an application duration of 4 seconds including multiple trains of biphasic bipolar pulses was delivered for each ablation site. This focal PFA catheter was designed with a bipolar distance of >0.3 cm, achieving <2500 V/cm that is a critical threshold for complete destruction of red blood cells.¹⁷ Furthermore, intravascular hemolysis was more common in atrial fibrillation patients treated with PFA compared with those treated with RF ablation.¹⁸ Considering the safety, we delivered PFA to each ablation site with the relatively lower output, so the lesions created in this study were not deeper than those created with the higher output and more repetitive applications. The deeper lesions might be achieved by this PFA catheter with application repetition, which needs further research for confirmation.

When RF energy is delivered to the RVOT, the catheter-tissue contact force is a primary driver of RF lesion size, and the reversed U-curve technique is warranted to treat PSC-derived VAs for making close contact with PSCs. However, this technique with excessive contact force is full of challenges with the risks of damage to the pulmonary valve leaflets, resulting in valvular dysfunction. Some research regarding PFA suggested that contact force is less important than tissue

Table 1 Depth of lesions created at LVOT and RVOT at 24 hours, 2 weeks, and 4 weeks after ablation

	24 hours after PFA	2 weeks after PFA	4 weeks after PFA
LVOT			
ASC	3.9 ± 0.9 mm	3.6 ± 1.1 mm	3.7 ± 1.0 mm
RVOT			
PSC	4.3 ± 1.2 mm	3.8 ± 0.6 mm	3.6 ± 0.4 mm
Free wall	3.8 ± 1.0 mm	3.4 ± 0.8 mm	3.5 ± 1.1 mm
Septal wall	3.6 ± 0.8 mm	3.3 ± 0.9 mm	2.9 ± 0.6 mm

Values are presented as mean \pm standard deviation.

ASC = aortic sinus cusp; LVOT = left ventricular outflow tract; PFA = pulsed field ablation; PSC = pulmonary sinus cusp; RVOT = right ventricular outflow tract.

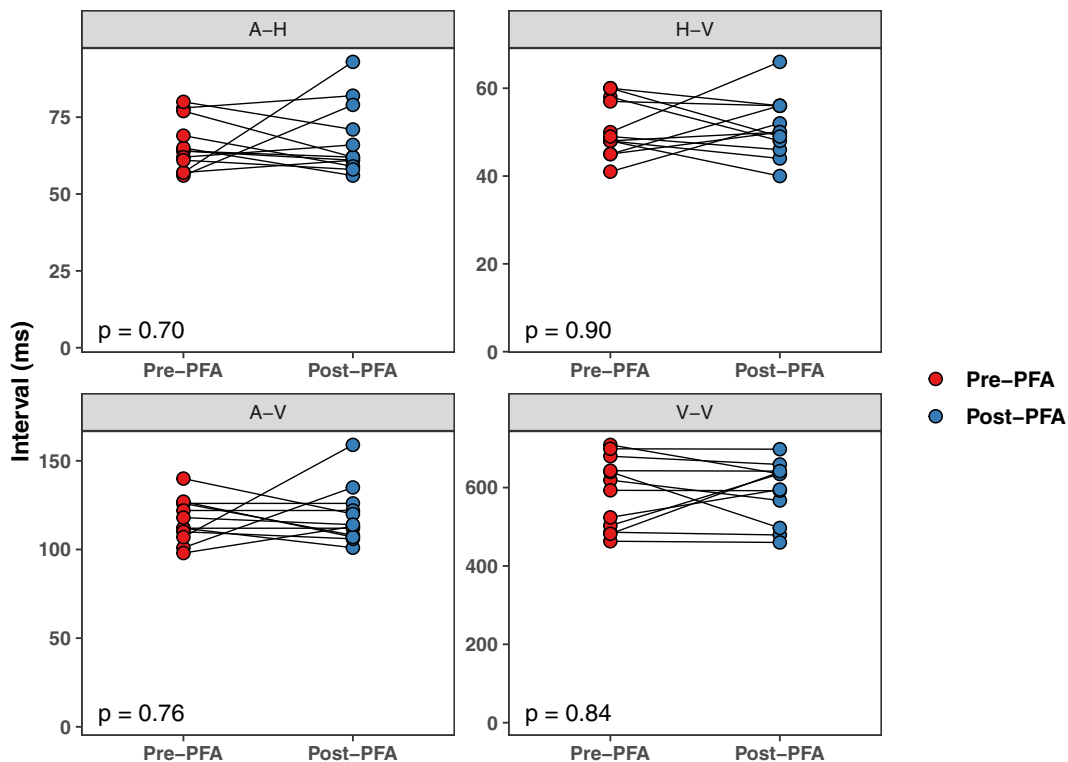


Figure 7

Changes in atrium to His (A-H), His to ventricle (H-V), atrioventricular (A-V), and ventricle to ventricle (V-V) intervals between pre and post pulsed field ablation (PFA).

contact,^{19,20} whereas recent studies have shown that the increased contact force had a critical impact on lesion dimensions when PFA was delivered through a focal point catheter or circular variable loop catheter.^{21,22} In this study, considering the safety, we achieved tissue contact by the novel PFA catheter to form a reversed U curve instead of enhancing contact force during PFA delivery. No valvular dysfunction assessed with ICE was observed after PFA delivery to the ASCs and PSCs. At 4 weeks after ablation, TEE showed no severe pulmonic regurgitation, with 1 minor pulmonic regurgitation. The causal link between PFA delivery and this regurgitation remains uncertain, highlighting the need for pre-ablation TEE comparisons for more conclusive assessments. Nevertheless, it was suggested that the novel PFA catheter with tissue contact achieved is likely to reduce the potential risk of damage to the pulmonary valve, offering a safe alternative for creating lesions near PSCs.

Catheter ablation inside ASCs, especially LCC and RCC, presents significant challenges because of their proximity to coronary artery ostia, raising the potential risk of coronary artery damage. In addition, the posterior aspect of RCC is adjacent to the central fibrous body that the His bundle penetrates, and the anterior aspect of RCC is close to the bifurcating atrioventricular bundle and the origin of the left bundle branch. Traditional RF ablations are likely to result in an atrioventricular block or left bundle branch block. However, these complications were not observed after PFA delivery to ASCs. Angiography confirmed no coronary artery damage, and electrocardiographic and electrophysiologic assessments showed no impact on atrioventricular conduction. Furthermore, histologic examination revealed a lack of collateral injury to ar-

terioles and nerves with the surrounding myocardium impaired and replaced, indicating the selectivity for myocardium compared with intramyocardial arterioles and nerves. Distinct thresholds for irreversible damage to different tissues might account for the selectivity of PFA,²³ laying a theoretical foundation for the safety of this PFA catheter used within ASCs.

PFA energy application to atrial tissue through the NCC offers a promising alternative for treating focal atrial tachycardia (AT), especially parahisian AT, given the proximity of the NCC to the atrial myocardium and His bundle.²⁴ In this study, histopathologic analysis of the NCC after ablation revealed continuous lesions on the epicardial aspect of the right atrium, with fibrous tissue replacement observed 4 weeks after ablation. Most important, no atrioventricular block was observed after PFA delivery to the ASCs. It was suggested that this focal point PFA catheter is likely to be a treatment alternative for NCC-related AT in terms of safety.

Study limitations

There are several limitations in this study. First, because of its preclinical nature, there could be differences in tissue response to PFA between healthy swine and humans. The final dosing of this PFA catheter used clinically for patients with VAs will likely differ from the one used in this study. Second, a single application per site was chosen to reduce complications, including atrioventricular block, valvular dysfunction, and coronary artery damage. Further studies are needed to evaluate the effects of multiple PFA applications. Finally, the small sample size with 4-week survival duration indicates the need for

more extensive and detailed studies to validate these initial findings comprehensively before adoption for clinical use.

Conclusion

In this preclinical study, the novel PFA catheter created durable lesions at PSCs and ASCs without causing collateral damage to coronary arteries, inducing atrioventricular block, or impairing valvular function. These findings indicate that PFA delivered by the focal point catheter could be used at the ventricular outflow tract safely.

Acknowledgments

We are sincerely grateful to Zhao Liu, Long Huang, and Yuntong Zhang for medical revision, editorial support, and animal study support.

Appendix

Supplementary data

Supplementary data associated with this article can be found in the online version at <https://doi.org/10.1016/j.hrthm.2024.10.059>.

Funding Sources: This work was supported by Capital Fund for Health Improvement and Research (2022-2Z-4036), National Natural Science Foundation of China (82371595), and Chinese Academy of Medical Sciences Innovation Fund for Medical Sciences (2021-I2M-1-063).

Disclosures: The authors have no conflicts of interest to disclose.

Authorship: All authors attest they meet the current ICMJE criteria for authorship.

Address reprint requests and correspondence: Dr Lihui Zheng, Arrhythmia Center, Fuwai Hospital, National Center for Cardiovascular Diseases, Chinese Academy of Medical Sciences and Peking Union Medical College, Beijing 100037, China. E-mail address: zhenglihui@263.net; or Dr Yan Yao, 167 Beilishi Rd, Xicheng District, Beijing 100037, China. E-mail address: ianyao@263.net.cn

References

- Zhang J, Tang C, Zhang Y, Su X. Pulmonary sinus cusp mapping and ablation: a new concept and approach for idiopathic right ventricular outflow tract arrhythmias. *Heart Rhythm* 2018;15:38–45.
- Liao Z, Zhan X, Wu S, et al. Idiopathic ventricular arrhythmias originating from the pulmonary sinus cusp: prevalence, electrocardiographic/electrophysiological characteristics, and catheter ablation. *J Am Coll Cardiol* 2015;66:2633–2644.
- Badhwar N, Scheinman MM. Idiopathic ventricular tachycardia: diagnosis and management. *Curr Probl Cardiol* 2007;32:7–43.
- Cronin EM, Bogun FM, Maury P, et al. 2019 HRS/EHRA/APHS/LAHS expert consensus statement on catheter ablation of ventricular arrhythmias. *Europace* 2019;21:1143–1144.
- Yamada T, Lau YR, Litovsky SH, et al. Prevalence and clinical, electrocardiographic, and electrophysiologic characteristics of ventricular arrhythmias originating from the noncoronary sinus of Valsalva. *Heart Rhythm* 2013;10:1605–1612.
- Edd JF, Horowitz L, Davalos RV, Mir LM, Rubinsky B. In vivo results of a new focal tissue ablation technique: irreversible electroporation. *IEEE Trans Biomed Eng* 2006;53:1409–1415.
- Rubinsky B, Onik G, Mikus P. Irreversible electroporation: a new ablation modality—clinical implications. *Technol Cancer Res Treat* 2007;6:37–48.
- Kaminska I, Kotulska M, Stecka A, et al. Electroporation-induced changes in normal immature rat myoblasts (H9C2). *Gen Physiol Biophys* 2012;31:19–25.
- Flachskampf FA, Wouters PF, Edvardsen T, et al. Recommendations for transoesophageal echocardiography: EACVI update 2014. *Eur Heart J Cardiovasc Imaging* 2014;15:353–365.
- Hahn RT, Abraham T, Adams MS, et al. Guidelines for performing a comprehensive transesophageal echocardiographic examination: recommendations from the American Society of Echocardiography and the Society of Cardiovascular Anesthesiologists. *J Am Soc Echocardiogr* 2013;26:921–964.
- Weyand S, Lobig S, Seizer P. First in human focal pulsed field ablation to treat an epicardial VT focus with an endocardial approach in non-ischemic cardiomyopathy. *J Interv Card Electrophysiol* 2023;66:1057–1058.
- Schmidt B, Chen S, Tohoku S, Bordignon S, Bologna F, Chun KR. Single shot electroporation of premature ventricular contractions from the right ventricular outflow tract. *Europace* 2022;24:597.
- Worck R, Haugdal MA, Johannessen A, Hansen ML, Ruwald MH, Hansen J. A case of safe and durable focal pulsed-field electroporation treatment of outflow tract premature ventricular contractions. *Heart Rhythm* 2023;4:463–465.
- Younis A, Tabaja C, Kleve R, et al. Comparative efficacy and safety of pulsed field ablation versus radiofrequency ablation of idiopathic LV arrhythmias. *JACC Clin Electrophysiol* 2024;10:1998–2009.
- Younis A, Buck E, Santangeli P, et al. Efficacy of pulsed field vs radiofrequency for the reablation of chronic radiofrequency ablation substrate: redo pulsed field ablation. *JACC Clin Electrophysiol* 2024;10:222–234.
- Yavin HD, Higuchi K, Sroubek J, Younis A, Zilberman I, Anter E. Pulsed-field ablation in ventricular myocardium using a focal catheter: the impact of application repetition on lesion dimensions. *Circ Arrhythm Electrophysiol* 2021;14:e010375.
- Peng W, Yue Y, Zhang Y, et al. Scheduled dosage regimen by irreversible electroporation of loaded erythrocytes for cancer treatment. *APL Bioeng* 2023;7:046102.
- Popa MA, Venier S, Mene R, et al. Characterization and clinical significance of hemolysis after pulsed field ablation for atrial fibrillation: results of a multicenter analysis. *Circ Arrhythm Electrophysiol* 2024;e012732.
- Mattison L, Verma A, Tarakji KG, et al. Effect of contact force on pulsed field ablation lesions in porcine cardiac tissue. *J Cardiovasc Electrophysiol* 2023;34:693–699.
- Howard B, Verma A, Tzou WS, et al. Effects of electrode-tissue proximity on cardiac lesion formation using pulsed field ablation. *Circ Arrhythm Electrophysiol* 2022;15:e011110.
- Younis A, Santangeli P, Garrott K, et al. Impact of contact force on pulsed field ablation outcomes using focal point catheter. *Circ Arrhythm Electrophysiol* 2024;17:e012723.
- Di Biase L, Marazzato J, Gomez T, et al. Application repetition and electrode-tissue contact result in deeper lesions using a pulsed-field ablation circular variable loop catheter. *Europace* 2024;26:euae220.
- Di Biase L, Diaz JC, Zhang XD, Romero J. Pulsed field catheter ablation in atrial fibrillation. *Trends Cardiovasc Med* 2022;32:378–387.
- Beukema RJ, Smit JJ, Adiyaman A, et al. Ablation of focal atrial tachycardia from the non-coronary aortic cusp: case series and review of the literature. *Europace* 2015;17:953–961.